PROCEEDINGS OF SCIENCE

Do we know eventually $\mathbf{p}(\mathbf{e})$?

B. Kämpfer[*†]
Forschungszentrum Dresden-Rossendorf, PF 510119, 01314 Dresden, Germany
E-mail: b.kaempfer@fzd.de

M. Bluhm, H. Schade, R. Schulze, D. Seipt
Forschungszentrum Dresden-Rossendorf, PF 510119, 01314 Dresden, Germany

A quasi-particle model is employed to derive from available lattice QCD calculations an equation of state useable in hydrodynamical simulations of the expansion stage of strongly interacting matter created in ultra-relativistic heavy-ion collisions. Various lattice results give an astonishing agreement of the pressure as a function of energy density at large energy densities supposed the pseudo-critical temperature is in the range 170 ± 15 MeV, while in the transition region the equation of state is not yet well constrained. Therefore, one can construct a family of equations of state by bridging the uncertain region from the uniquely given high-energy density region part to a hadronic equation of state by suitable interpolation together with the extrapolation to non-zero baryon density by means of the quasi-particle model. We present a series of tests of the model, discuss the chiral extrapolation and the role of Landau damping. We also briefly sketch the path of cosmic matter in the early universe in the phase diagram.

Critical Point and Onset of Deconfinement - 4th International Workshop
July 9 - 13, 2007
Darmstadt, Germany

[*]Speaker.
[†]also at TU Dresden, 01062 Dresden, Germany

PoS(CPOD07)007

1. Introduction

The equation of state of strongly interacting matter is a central issue for understanding and modelling the adiabatic path of cosmic matter of the expanding universe (hot QCD), the expansion of matter created in ultra-relativistic heavy-ion collisions (hot and medium-dense QCD), and compact stars (dense QCD). Intimately related is the phase diagram of strongly interacting matter with challenges like the nature and localization of the deconfinement transition and the occurrence of a critical point on the phase border curve. Ab initio calculations evaluating observables which quantify these notions are still in progress. It is, therefore, opportune to employ at this stage of insight in QCD appropriate models to interpolate and extrapolate the various pieces of knowledge aiming at delivering, e.g., a useable equation of state.

The tool employed here is the quasi-particle model developed in [1]. We are going to address the question whether a unique equation of state, applicable for ultra-relativistic heavy-ion collisions, is at our disposal. Furthermore, we report on a few recent improvements of the model.

Our paper is organized as follows. In section 2 we review the quasi-particle model, which is exploited in section 3 to derive an equation of state suitable for predictions for heavy-ion collisions at RHIC and LHC energies. The possibility to extend the model by explicitly accounting for the critical point is addressed in section 4. Partial improvements (such as an attempt of chiral extrapolation, and inclusion of Landau damping and other plasma excitations, and imaginary chemical potential) are briefly reported in section 5. Finally, we comment on the adiabatic path of strongly interacting matter in the expanding universe (section 6).

2. Quasi-particle model

The present basic version of the employed quasi-particle model is related to QCD as follows [2]: (i) two-loop Φ functional which results in one-loop self-energies, (ii) neglect of imaginary parts of self-energies (and, via Dyson's relation, also in propagators) as well as neglect of (anti)plasmino and longitudinal gluon excitations, (iii) use of approximate energy (ω) - momentum (k) relations of quasi-particle excitations

$$\omega_T^2 \;=\; k^2+m_\infty^2, \quad m_\infty^2=\frac{1}{12}\left([2N_c+N_f]T^2+\frac{N_c}{\pi^2}N_f\mu_q^2\right)G^2(T,\mu_q), \tag{2.1}$$

$$\omega_q^2 \;=\; k^2+m_q^2+2m_qM_+ +2M_+^2, \quad M_+^2=\frac{N_c^2-1}{16N_c}\left(T^2+\frac{\mu_q^2}{\pi^2}\right)G^2(T,\mu_q) \tag{2.2}$$

for transverse gluons (T) and quarks (q), where (iv) the effective coupling G^2 obeys Peshier's equation $a_T\frac{\partial G^2}{\partial T}+a_{\mu_q}\frac{\partial G^2}{\partial \mu_q}+a_GG^2=0$ with coefficients $a_{\mu_q,T,G}$ given in [2, 3], once $G^2(T,\mu_q=0)$ in the parametrization

$$G^2(T)=\begin{cases} G^2_{\rm 2loop}(\xi), \quad \xi=\lambda\frac{(T-T_s)}{T_c},\ T\geq T_c \\ G^2_{\rm 2loop}(T_c)+b(1-\frac{T}{T_c}), \qquad T<T_c \end{cases} \tag{2.3}$$

is adjusted to lattice data. ($G^2_{\rm 2loop}$ is the two-loop running QCD coupling, however, with argument ξ.) The expressions for baryon and entropy density look like the standard statistical integrals,

however, with state-dependent mass gaps m_∞^2 and $M^2 = m_q^2 + 2m_q M_+ + 2M_+^2$ for gluons and quarks. For quarks, the existence of a mass gap related to M_+ emerges now from lattice simulations in the quenched approximation [4]. The dependence of the latter ones on the quark chemical potential μ_q, beyond the dependence on the temperature T, is called the BKS effect in [5].

The model has been tested against various sets of lattice QCD results for N_f flavors and $N_c = 3$ colors, see [1, 6]. A recent extension of the model towards two independent chemical potentials $\mu_{u,d}$ allows the calculation of quark number and isovector susceptibilities as well as diagonal and off-diagonal susceptibilities and their respective Taylor expansion coefficients

$$\frac{\chi_q}{T^2} = 2c_2 + 12c_4 \left(\frac{\mu_q}{T}\right)^2 + \cdots, \tag{2.4}$$

$$\frac{\chi_I}{T^2} = 2c_2^I + 12c_4^I \left(\frac{\mu_I}{T}\right)^2 + \cdots, \tag{2.5}$$

$$\frac{\chi_{uu}}{T^2} = 2c_2^{uu} + 12c_4^{uu} \left(\frac{\mu_q}{T}\right)^2 + \cdots, \tag{2.6}$$

$$\frac{\chi_{ud}}{T^2} = 2c_2^{ud} + 12c_4^{ud} \left(\frac{\mu_q}{T}\right)^2 + \cdots, \tag{2.7}$$

being second-order derivatives of the grand thermodynamical potential. The light-quark chemical potentials are decomposed as $\mu_q = \frac{1}{2}(\mu_u + \mu_d)$ and $\mu_I = \frac{1}{2}(\mu_u - \mu_d)$, where μ_I denotes the isospin chemical potential. A comparison with lattice QCD results is displayed in Fig. 1. This additional test provides further confidence in the model.

3. Hydrodynamics for RHIC and LHC

Due to various differences of the implementation of QCD on a space-time grid to evaluate the equation of state for $N_f = 2+1$ flavors, some differences are obvious, as demonstrated in the left panel of Fig. 2. The surprise however is that a translation of these differing lattice results for the scaled pressure p as a function of the scaled temperature into the relation of pressure as a function of energy density e by means of the above quasi-particle model provides a unique equation of state at large energy densities. In this respect one may arrive at the conclusion that the equation of state $p(e)$ in the form pressure vs. energy density is eventually at our disposal for large values of e. As the calculations exhibited in the left panel of Fig. 2 are for $\mu_q = 0$ we use again our quasi-particle model to supplement the baryon density dependence. The successful tests of the baryon density dependence of two-flavour QCD in [6] and the in the previous section provide confidence in the reliable extrapolation to $\mu_q > 0$.

The transition region, corresponding to temperatures of the oder of the pseudo-critical temperature, $T \sim T_c$, however, seems not yet to be settled. We construct, therefore, a family of equations of state by interpolating from the unique high-density QCD part to a low-density hadron resonance part. The resulting equation of state is used for the hydrodynamical calculation of transverse momentum ($p_\perp$) spectra and azimuthal asymmetry v_2 of various hadron species for RHIC and future LHC energies. Keeping initial and freeze-out conditions fixed, the spectra and $v_2(p_\perp)$ show some dependence on the shape of $p(e)$ in the region around T_c. This may enable further constraints on the equation of state by comparison with experimental data from RHIC, a programme already pursued by [11]. For results and details the interested reader is referred to [12, 13].

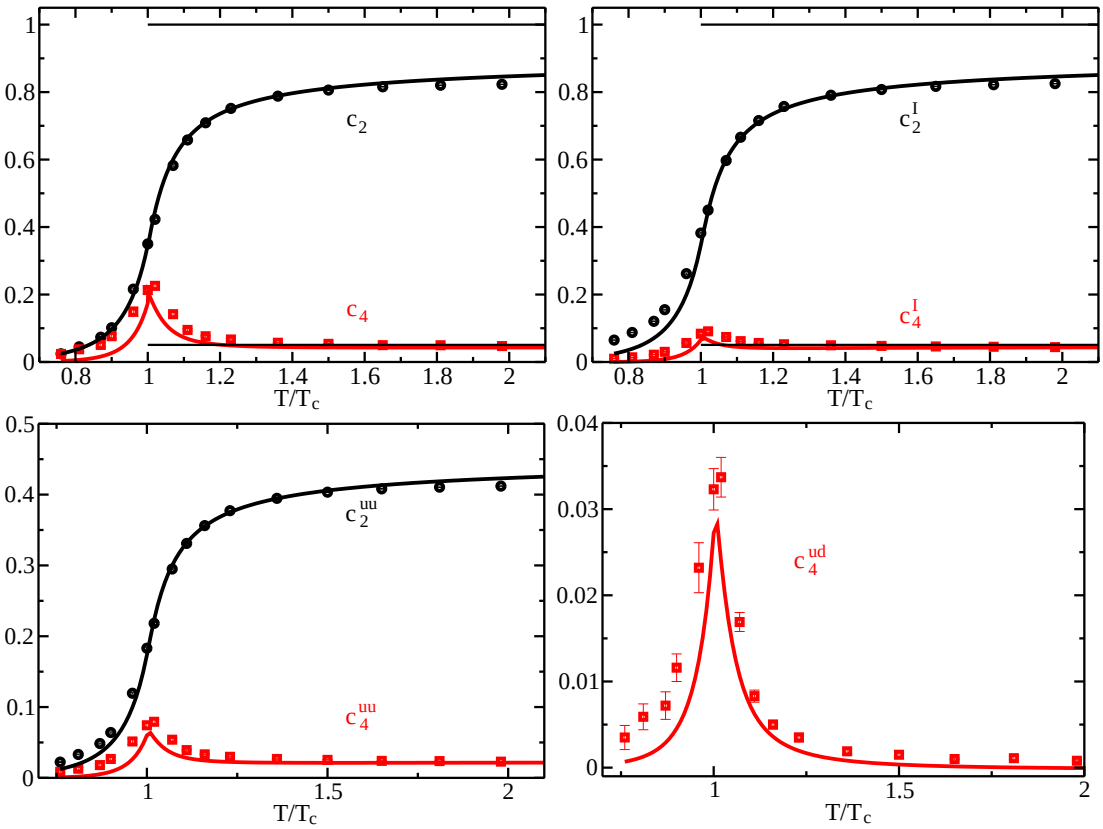

Figure 1: Taylor expansion coeffi cients for susceptibilities. Lattice QCD data from [7]. Straight lines for $T > T_c$ depict here and in the following the perturbative results.

4. Including the critical point

The change of the slope of the employed effective coupling (2.3) at T_c is primarily responsible for the pronounced structures observed in c_4, c_4^I, c_4^{uu} and c_4^{ud} in Fig. 1. While the rise for $T \geq T_c$ close to T_c is dictated by the perturbative behavior of G^2, the decrease for $T < T_c$ is due to the conversion into the linear temperature dependence. Such a change in the curvature behavior was also found by solving Dyson-Schwinger equations in Coulomb gauge [14]. This behavior may be interpreted as an indication of some criticality in agreement with lattice QCD results, nonetheless, one can further extend the model by including explicitly a singular part which belongs to the universality class of the three-dimensional Ising model. In such a way the conjectured QCD critical point can be modelled without destroying the agreement with the available lattice QCD results [7]. Such a phenomenological procedure, first proposed in [15], is described in [16]. It offers the opportunity to study various observables within a hydrodynamical framework for matter states in the vicinity of the critical point, similar to first investigations along this line in [17].

5. Recent developments

The severe approximations described in beginning of section 2 are matter of ongoing investigations. Here we describe some of such studies.

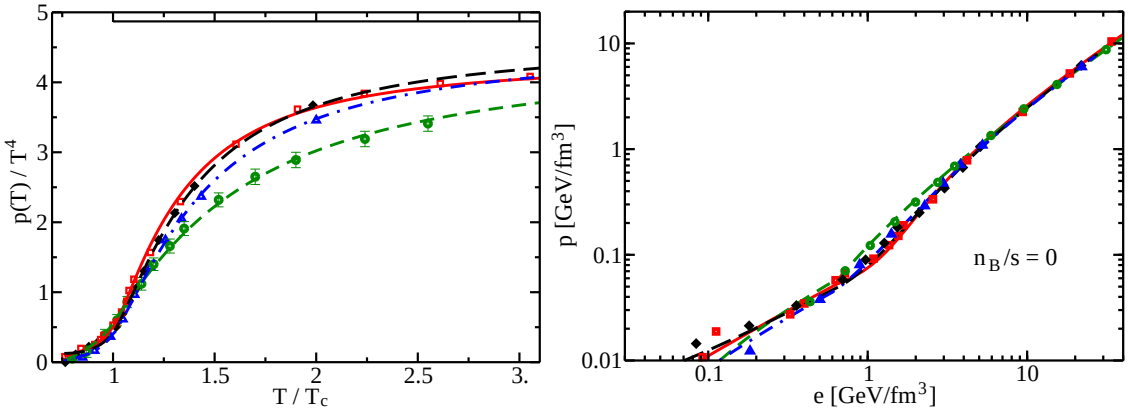

Figure 2: Left panel: Scaled pressure as a function of scaled temperature (quasi-particle model [curves] adjusted to various selected lattice QCD data [symbols] from [8, 9, 10]). Right panel: Resulting equation of state in the form of pressure p vs. energy density e when using the scale $T_c = 170$ MeV. The curves are robust against variations in T_c for small and large e. Only in the transition region 1 GeV/fm^3 $\leq$ e $\leq$ 5 GeV/fm^3 noticeable differences of at most 20% arise when modifying T_c by ± 10 MeV.

5.1 Chiral extrapolation

Lattice performances require still fairly large quark masses. Given the form of the approximated quark dispersion relation (2.2) with lattice mass parameter m_q one can attempt to perform a chiral extrapolation by putting $m_q \to 0$. The result of such a procedure is exhibited in Fig. 3. The semi-quantitative agreement with new lattice QCD results with smaller quark masses supports the idea that an implicit dependence of G^2 on quark masses is weak.

A calculation of the quasi-particle dispersion relations based on one-loop self-energies with finite quark masses in Feynman gauge [19] renders the above simplified expressions (2.1) and (2.2) at $\mu_q = 0$ into

$$\omega_T^2 = k^2 + m_\infty^2, \quad m_\infty^2 = \frac{1}{6} G^2 T^2 \left(N_c + \frac{1}{2} \sum_q \mathscr{I}(\frac{m_q}{T}) \right), \tag{5.1}$$

$$\omega_q^2 = k^2 + m_q^2 + 2M_+^2, \quad M_+^2 = \frac{1}{6} G^2 T^2 \left(\frac{2}{3} + \frac{1}{3} \mathscr{I}(\frac{m_q}{T}) \right) \tag{5.2}$$

with the asymptotic representation for small values of m_q/T

$$\mathscr{I}(x) = 1 + a_2 x^2 + a_L x^2 \log x^2 + a_4 x^4 + \cdots, \tag{5.3}$$

$$a_2 = -\frac{3}{\pi^2}(\log \pi + \frac{1}{2} - \gamma_E), \tag{5.4}$$

$$a_L = \frac{3}{2\pi^2}, \tag{5.5}$$

$$a_4 = -\frac{21}{16\pi^4}\xi(3). \tag{5.6}$$

The asymptotic masses m_∞^2 and $M_\infty^2 = m_q^2 + 2M_+^2$ are found to be gauge invariant quantities [19]. (5.1) and (5.2) as well as improved dispersion relations offer the possibility of sound chiral extrapolations.

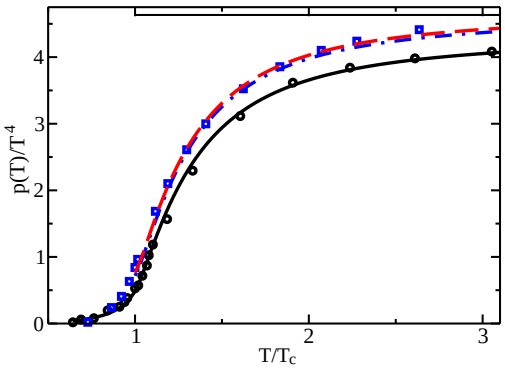

Figure 3: Scaled pressure as a function of scaled temperature. Symbols depict lattice QCD data for $2+1$ flavors from [8] (full circles, $m_{u,d} = 0.4T$, $m_s = T$) and [18] (squares, $m_\pi = 220$ MeV). The black solid curve employs quark masses as on the lattice, the red dashed curve is for the chiral limit, while the blue dash-dotted curve uses $m_{u,d} = 0.024T$ MeV and $m_s = 0.24T$ MeV.

5.2 Landau damping

While the quasi-particle model as outlined in section 2 describes fairly well the Taylor expansion coefficients of [7], thus establishing the correct μ_q dependence for small μ_q, it exhibits an ostensible ambiguity at larger μ_q: By solving Peshier's equation to determine $G^2(T,\mu_q)$, the characteristic curves emerging from the vicinity of T_c cross each other at larger μ_q. As indicated in [20], including the imaginary parts of HTL/HDL self-energies cures this unpleasant feature. A detailed study [21] shows that the negative longitudinal gluon and (anti)plasmino contributions to the entropy density allow for a better adjustment of the model to lattice QCD data [18] leading to less crossings. However, the complete cure of crossings is due to Landau damping terms within Peshier's equation.

5.3 Imaginary chemical potential

The notorious sign problem of the fermionic determinant is avoided for a purely imaginary chemical potential (see [22] for recent reviews), where QCD recovers the center symmetry giving rise to the Roberge-Weiss periodicity [23]. Our quasi-particle model, as described in section 2 can be applied accordingly by the replacement of baryo-chemical potential $\mu_q \to i\mu_i \equiv \mu_B/3$. This replacement flips signs at a few important points in the equations for the thermodynamic quantities, the self-energies and the Peshier equation. For instance, m_∞^2 and M_+^2 in (2.1) and (2.2) render to

$$m_\infty^2 = \frac{1}{12}\left([2N_c+N_f]T^2 - \frac{N_c}{\pi^2}N_f\mu_i^2\right)G^2(T,i\mu_i), \tag{5.7}$$

$$M_+^2 = \frac{N_c^2-1}{16N_c}\left(T^2 - \frac{\mu_i^2}{\pi^2}\right)G^2(T,i\mu_i)\,. \tag{5.8}$$

This comprises an additional sensible test, even if the truncation of QCD by the chosen Φ functional, the approximated HTL/HDL self-energies and the neglect of imaginary parts in the self-energies discards the center symmetry of full QCD with imaginary chamical potential. A comparison with lattice QCD results is displayed in Fig. 4. In particular, the importance of the BKS-effect [5, 24] for the successful description of the observed pattern in the quark number density can be

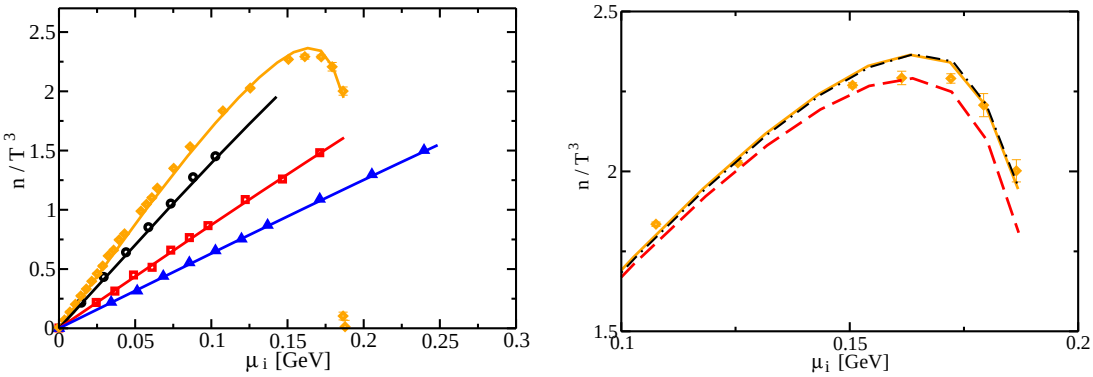

Figure 4: Left: scaled quark number density as a function of imaginary chemical potential for various temperatures. Symbols denote lattice QCD data from [24] for $T = 1.1, 1.5, 2.5, 3.5\,T_c$ (diamonds, circles, squares and triangles, respectively). Right: test of the BKS effect for $T = 1.1\,T_c$ as explained in the text.

studied as depicted in the rigth panel of Fig. 4. For example, one could neglect the terms explicitly depending on μ_i in the quasi-particle dispersion relations with (5.7) and (5.8) which enter the thermodynamic expression of the quark number density but leaving Peshier's equation unchanged. This renders the found results only at larger values of μ_i (dashed line). Thermodynamic consistency, nonetheless, requires in addition corresponding changes in Peshier's equation resulting in negligible deviations (dash-dotted line) from the results shown in the left panel of Fig. 4. Thus, one may conclude that an explicit μ_i-dependence of the quasi-particle's effective masses is not necessarily required for describing these lattice QCD results [24]; instead the μ_i-dependence of G^2 matters.

6. Strongly interacting matter in the expanding universe

The WMAP data on the fluctuations of the cosmic microwave background deliver a value of 6.1×10^{-10} (ΛCDM model and 3-year WMAP-data-only [25]) for the ratio of baryons to photons. Assuming adiabaticity and baryon conservation this translates into 2.3×10^{-11} for the inverse of the specific entropy of baryons. The corresponding adiabatic path is displayed in the temperature–baryo-chemical potential plane in Fig. 5 (for plots in log scales cf. [26, 27]). A similar path has been reported in [28], where also charge neutrality and lepton conservation are implemented. Intriguing is the sharp turn from a region of small baryo-chemical potential, $\mu_B/T \ll 1$, to large one, $\mu_B/T \gg 1$, at temperature scale slightly below 50 MeV. On the displayed path the time varies from 1 μsec to 0.1 sec, and the universe is radiation dominated. At $T > T_c$ the strongly interacting (deconfined) matter dominates over the electro-weak matter, while at $T < T_c$ the electro-weak matter dominates for a long time until recombination. "Dominating" means here that the contribution to energy density, pressure or entropy density exceeds the other contributions.

7. Summary

In summary we survey the status of our quasi-particle model and compare it with lattice QCD

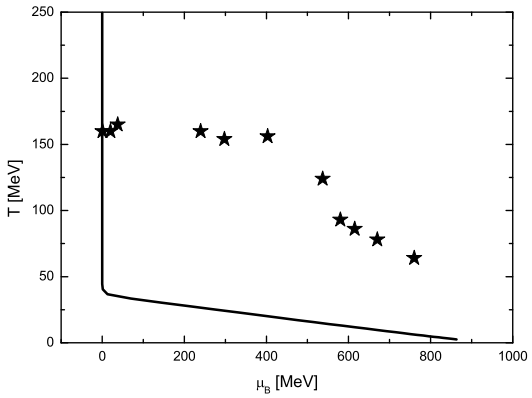

Figure 5: Adiabatic path of cosmic matter for inverse specifi c entropy of 2.3×10^{-11}, assuming about 10 degrees of freedom (photons, standard model neutrinos, electrons) for the entropy density. The asterisks depict chemical freeze-out points from [29] (table 2–upper part, and a LHC estimate mentioned in the text there).

data. We argue that the equation of state in the form pressure as a function of energy density, $p(e)$, is eventually known at large energy densities and small baryo-chemical potential.

Acknowledgements

The authors thank P. Braun-Munzinger, F. Karsch, E. Laermann, M. P. Lombardo for useful discussions. The work is supported by BMBF 06DR136, GSI DRKAM, and EU I3HP.

References

[1] A. Peshier, B. Kämpfer, O. P. Pavlenko and G. Soff, Phys. Lett. B **337**, 235 (1994); Phys. Rev. D **54**, 2399 (1996). A. Peshier, B. Kämpfer and G. Soff, Phys. Rev. C **61**, 045203 (2000) [hep-ph/9911474]; Phys. Rev. D **66**, 094003 (2002) [hep-ph/0206229].

[2] M. Bluhm, B. Kämpfer, R. Schulze and D. Seipt, Eur. Phys. J. C **49**, 205 (2007) [hep-ph/0608053].

[3] M. Bluhm, Diploma Thesis, Technische Universität Dresden, August 2004.

[4] F. Karsch and M. Kitazawa, [arXiv:0708.0299 [hep-lat]]

[5] J. Liao and E. V. Shuryak, Phys. Rev. D **73**, 014509 (2006) [hep-ph/0510110].

[6] M. Bluhm, B. Kämpfer and G. Soff, Phys. Lett. B **620**, 131 (2005) [hep-ph/0411106].

[7] C. R. Allton, S. Ejiri, S.J. Hands, O. Kaczmarek, F. Karsch, E. Laermann and C. Schmidt, Phys. Rev. D **68**, 014507 (2003) [hep-lat/0305007]. C. R. Allton, M. Döring, S. Ejiri, S. J. Hands, O. Kaczmarek, F. Karsch, E. Laermann and K. Redlich, Phys. Rev. D **71**, 054508 (2005) [hep-lat/0501030].

[8] F. Karsch, K. Redlich and A. Tawfi k, Eur. Phys. J. C **29**, 549 (2003) [hep-ph/0303108]; Phys. Lett. B **571**, 67 (2003) [hep-ph/0306208].

[9] C. Bernard *et al.*, Phys. Rev. D **55**, 6861 (1997) [hep-lat/9612025]. C. Bernard *et al.*, PoS **LAT2005**, 156 (2005) [hep-lat/0509053].

[10] Y. Aoki, Z. Fodor, S. D. Katz and K. K. Szabo, JHEP **0601**, 089 (2006) [hep-lat/0510084].

[11] P. Huovinen, Nucl. Phys. A **761**, 296 (2005) [nucl-th/0505036]. P. Huovinen and P. V. Ruuskanen, Ann. Rev. Nucl. Part. Sci. **56**, 163 (2006) [nucl-th/0605008].

[12] M. Bluhm, B. Kämpfer, R. Schulze, D. Seipt and U. Heinz, [arXiv:0705.0397 [hep-ph]].

[13] M. Bluhm, B. Kämpfer and U. Heinz, [arXiv:0708.1653 [hep-ph]].

[14] D. Epple, H. Reinhardt and W. Schleifenbaum, Phys. Rev. D **75**, 045011 (2007) [hep-th/0612241].

[15] C. Nonaka and M. Asakawa, Phys. Rev. C **71**, 044904 (2005) [nucl-th/0410078].

[16] B. Kämpfer, M. Bluhm, R. Schulze, D. Seipt and U. Heinz, Nucl. Phys. A **774**, 757 (2006) [hep-ph/0509146]. M. Bluhm and B. Kämpfer, PoS **CPOD2006**, 004 (2006) [hep-ph/0611083].

[17] K. Paech, H. Stoecker and A. Dumitru, Phys. Rev. C **68**, 044907 (2003) [nucl-th/0302013]. K. Paech and A. Dumitru, Phys. Lett. B **623**, 200 (2005) [nucl-th/0504003].

[18] C. Schmidt, PoS **CPOD2006**, 002 (2006) [hep-lat/0701019].

[19] D. Seipt, Diploma Thesis, Technische Universität Dresden, May 2007.

[20] P. Romatschke, [hep-ph/0210331]. A. Rebhan and P. Romatschke, Phys. Rev. D **68**, 025022 (2003) [hep-ph/0304294].

[21] R. Schulze, Diploma Thesis, Technische Universität Dresden, June 2007.

[22] M. P. Lombardo, Prog. Theor. Phys. Suppl. **153**, 26 (2004) [hep-lat/0401021]. O. Philipsen, PoS **LAT2005**, 016 (2006); PoS **JHW2005**, 012 (2006) [hep-lat/0510077].

[23] A. Roberge and N. Weiss, Nucl. Phys. B **275**, 734 (1986).

[24] M. D'Elia and M. P. Lombardo, Phys. Rev. D **70**, 074509 (2004) [hep-lat/0406012]. M. D'Elia, F. Di Renzo and M. P. Lombardo, [arXiv:0705.3814 [hep-lat]].

[25] D. N. Spergel et al., Astrophys. J. Suppl. **170**, 377 (2007) [astro-ph/0603449]

[26] B. Kämpfer and M. Bluhm, J. Phys. G **31**, 1141 (2005) [hep-ph/0410396].

[27] H. Schade and B. Kämpfer, [arXiv:0705.2003 [hep-ph]].

[28] P. Braun-Munzinger and J. Wambach, Phys. J. **5**, 41 (2006). P. Braun-Munzinger and J. Stachel, Nature **448**, 302 (2007).

[29] A. Andronic, P. Braun-Munzinger and J. Stachel, Nucl. Phys. A **772**, 167 (2006) [nucl-th/0511071].